



Measuring the near-target neutron field of a D–D fusion facility with the novel NCT-WES spectrometer

R. Bedogni¹, A. Calamida¹, A. Fontanilla¹, A. I. Castro Campoy¹, T. Napolitano¹, C. Cantone¹, E. Mafucci^{2,3}, V. Monti^{2,3}, S. Altieri^{4,5}, J. M. Gomez-Ros⁶, M. Pillon⁷, A. Pietropaolo^{7,a} 

¹ Istituto Nazionale di Fisica Nucleare, Laboratori Nazionali di Frascati, Via Enrico Fermi 40, 00044 Frascati, Italy

² Università degli Studi di Torino, Via P. Giuria 1, 10125 Turin, Italy

³ INFN, Sezione di Torino, Via P. Giuria 1, 10125 Turin, Italy

⁴ Università degli Studi di Pavia, Via Bassi, 6, 27100 Pavia, Italy

⁵ INFN Sezione di Pavia, Via Bassi, 6, 27100 Pavia, Italy

⁶ CIEMAT, Av. Complutense 40, 28040 Madrid, Spain

⁷ Department of Fusion and Technologies for Nuclear Safety and Security, ENEA, Frascati (Roma), Italy

Received: 27 February 2022 / Accepted: 5 June 2022

© The Author(s) 2022

Abstract A new directional neutron spectrometer called NCT-WES (Neutron Capture Therapy Wide Energy Spectrometer) was recently developed within the INFN ENTER_BNCT project. This device constitutes a more compact and portable alternative to state-of-the-art directional neutron spectrometers. The device was used for the first time to characterise the near-target field produced by an accelerator-driven D–D fusion neutron source. NCT-WES operates as a “parallelised” Bonner spheres spectrometer, embedding six semiconductor-based thermal neutron detectors in a cylindrical moderator. Owing on a cylindrical collimating aperture, the device exhibits sharply directional response. To account for the non-uniform irradiation condition experienced in the near-target field, a dedicated NCT-WES response matrix was developed. The neutron spectrum at 0° from the D–D neutron target, determined by means of the FRUIT unfolding code, is coherent with that previously derived with Bonner spheres. NCT-WES proved to be a promising device for angular spectrometric characterisation of neutron-emitting targets.

1 Introduction

Compact accelerator-driven D–D and D–T fusion neutron sources are a fundamental research tool in neutron science, and their application ranges from fusion science to radiobiology and nuclear medicine [1]. Featuring a point-like neutron-emitting target, these sources are often used at short distance to achieve high values of fluence rate. Due to the combination of the kinematics and the angular distribution of the fusion cross-section, this near-target field can be highly anisotropic, especially for D–D sources [1]. Therefore, combined angular and spectrometric measurements are desirable to better characterise these facilities. The directional spectrometer NCT-WES (Neutron Capture Therapy Wide Energy Spectrometer) was developed within the INFN project ENTER_BNCT to operate rapid neutron spectrum measurements over the energy range from thermal up to 20 MeV neutrons. As the other single moderator neutron spectrometers created by the same collaboration [2–5], NCT-WES [6] offers the advantages of a Bonner sphere spectrometer (BSS) [5] in terms of high sensitivity, easy operation and wide energy range, but it requires only one exposure to examine all energy components of the field. The spectrum is obtained by processing the data from these detectors, together with the response matrix and the uncertainties, with a traditional few-channel unfolding code. NCT-WES is the low-energy evolution of CYSP (cylindrical spectrometer) [2, 7, 8], the first directional single-moderator spectrometer based on a collimated cylinder. CYSP is as heavy as 120 kg, as it includes enough attenuating material (polyethylene, borated rubber and lead) to respond from thermal up to GeV neutrons. Compared to CYSP, NCT-WES is lighter and more portable (35 kg), and its upper energy limit is about 20 MeV. This device was chosen to characterise the near-target 3-MeV neutron field produced at 0° from the target of the ENEA Frascati Neutron generator in D–D mode [9]. With a neutron yield in the order 3×10^8 – 4×10^8 s^{−1} and the target-to-spectrometer distance 136 cm, the counting rate in the spectrometer internal detectors was as high as 20–30 s^{−1}. Although the application of the shadow-cone technique required a double exposure, the whole spectrometry measurements took less than 1 h.

^a e-mail: antonino.pietropaolo@enea.it (corresponding author)

Fig. 1 Picture of the set-up for the near-target field measurements at the FNG facility: 1 is the NCT-WES, 2 is the shadow cone and 3 is the FNG neutron-emitting target

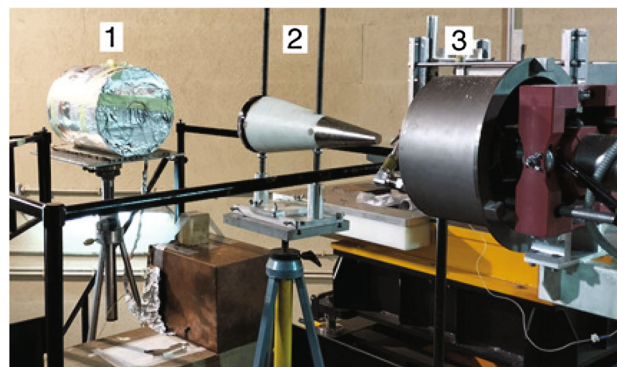
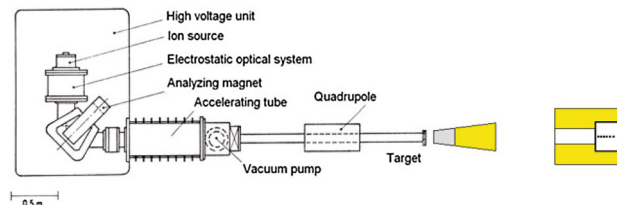


Fig. 2 Schematic layout of the FNG facility with the main components and the shadow cone and the NCT-WES device



2 The NCT-WES device

NCT-WES is a polyethylene cylinder with 36 cm diameter and 41.5 cm height (label 1 in Fig. 1). The cylindrical collimating aperture is 19.5 cm in length and 12 cm in diameter and is internally lined with borated rubber. Further details are given elsewhere [6]. Six thermal neutron detectors are located at different depths along the cylindrical axis of the device, beyond the collimator. The centre of the shallowest detector (detector 1) is located at 20.2 cm from the spectrometer front face, whilst the deepest one (detector 6) is located at 28.1 cm. The distance from the neutron target (label 3 in Fig. 1) to the spectrometer front face was 136 cm, so that the distance from the neutron target to the internal detectors ranged from 156.2 cm to 164.1. This 8-cm detector displacement is significant if compared to the source-to-spectrometer distance of 136 cm. Thus, the “broad parallel beam” response matrix [10] could not be used, and geometry-specific response matrix was calculated. The D–D fusion source exhibits anisotropy in terms of intensity and energy distribution of the neutron emission [11]. At 136 cm distance, the NCT-WES collimated aperture, 12 cm in diameter, only covers an angle of 5° . Based on the literature [11], both angular emission and energy distribution can be considered as uniform over this angle. The measurement set-up was assembled at 4 m height from the floor of the $20 \times 20 \times 9 \text{ m}^3$ FNG hall. The shadow-cone technique [12] was used to correct for the room-scattered field. The shadow-cone (label 2 in Fig. 1) had minimum and maximum diameters 3 cm and 19 cm, respectively, and it was positioned with the iron end at 10 cm from the target. The spectrometer front face was obscured by the cone with a shadowing ratio 1.9, in agreement with the ISO criterion [12]. The irradiation set-up is schematised in Fig. 2, where also the FNG layout is shown. The NCT-WES internal thermal neutron detectors are called TNPD (thermal neutron pulse detector). These are 1-cm^2 windowless $p-i-n$ diodes made sensitive to thermal neutrons through deposition of about $30 \mu\text{m}$ of ^6LiF on the sensitive face [13, 14]. TNPDs are connected to a customised nuclear spectroscopy chain formed by a CREMAT CR110 charge preamplifier, a CR200 shape amplifier (shaping time $2 \mu\text{s}$) and a digitiser. As explained in Ref. [14], the genuine neutron-induced events are separated from those induced by photons by comparing the pulse height with a threshold, fixed to 0.6 V. FNG operated in D–D mode. An accelerated deuteron beam with energy between 245 and 260 keV impinged on a titanium-coated copper target where deuterium atoms are implanted. The deuterium current ranged between 30 and $35 \mu\text{A}$, leading to a source term between 3×10^8 and $4 \times 10^8 \text{ s}^{-1}$. The expected monochromatic neutron energy in the forward direction was 3.1 MeV. The beam was monitored by means of a charged particle silicon detector, placed at about 179° with respect to the primary beam and counting the ^3He particles from the $^2\text{H}(^2\text{H},n)^3\text{He}$ fusion reactions.

3 NCT-WES response matrix

The spectrometer was modelled using MCNP 6 [15], including an accurate description of the TNPD internal detectors. The detector reading, intended as the number of pulses from alpha or tritium particles escaping the ^6LiF radiator and reaching the silicon active layer, was assumed to be proportional to the number of (n, t) capture reactions in the ^6LiF radiator. A point source located at 136 cm from the spectrometer front face was included in the simulation model, leading to the determination of the spectrometer response in terms of counts per emitted neutron as a function of the neutron energy and the detector position. The disadvantage of such approach is that the response matrix varies as the source-to-spectrometer distance varies. The ENDF/B-VIII [16] neutron

Fig. 3 NCT-WES response matrix in terms of expected number of measured pulses in the TNPD, per emitted neutron, as a function of the energy and the detector position. $R(E)$ represents the counts per emitted neutron at 136 cm from the front face. P_i ($i = 1, 6$) indicates the detector position inside the NCT-WES

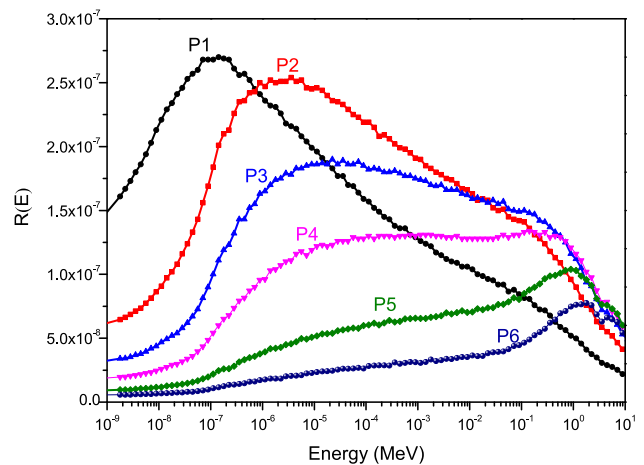
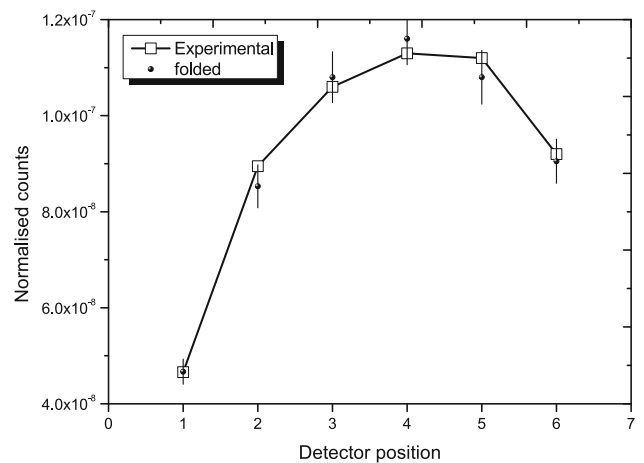


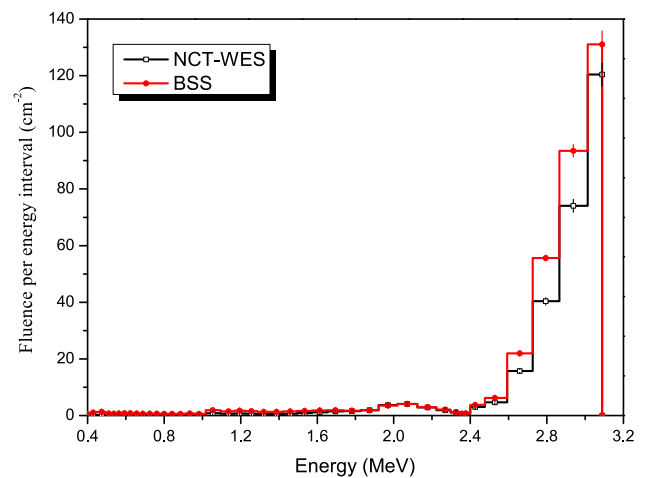
Fig. 4 Experimental and “folded” normalised counts in the NCT-WES internal detectors exposed to the un-collided field (total field—shadow-cone). Only the uncertainties on the simulated profile (about 5%) are reported for a better readability. Line is only a guide for the eye. The centre of the shallowest detector is located at 0.72 cm from the end of the collimator. Detectors’ spacing (centre to centre) is 1.3 cm from the 1st to the 4th, and 2 cm from the 4th to the 6th. The detectors are parallelepiped with external dimensions of 0.32 cm \times 1.5 cm \times 1.3 cm and are connected through a 2-mm-diameter coaxial cable



cross-section libraries below 20 MeV and room-temperature cross-section tables in polyethylene, $S(\alpha, \beta)$, were used. The scored quantity was the number of (n, t) events in the TNPD ${}^6\text{LiF}$ radiator. This was converted into a number of measurable pulses by applying a previously measured scaling factor $F = (0.238 \pm 0.006)$ [6], defined as the number of measurable pulses per (n, t) capture reaction in the ${}^6\text{LiF}$ radiator of the TNPD. The response matrix is shown in Fig. 3, where the labels “P1” to “P6” indicate the detector positions, from the shallowest to the deepest one. The maximum in the response functions shifts from fractions of eV (P1) to few MeV (P5 and P6).

4 Data collection and analysis

Data acquisition time for the shadow-cone measurements was of order 1200 seconds, allowing the achievement of statistical uncertainties better than 2% on the number of counts in TNPDs above the 0.6 V threshold. The total field measurement lasted the same time, with statistical uncertainties better than 1%. For both “total field” and “shadow-cone” measurements, the counts in the TNPD were normalised to the ${}^3\text{He}$ counter reading. This is termed “normalised count”. For each detector position, the normalised count due to the un-collided component was evaluated by subtracting the shadow-cone normalised count from the total field normalised count. If compared to the un-collided component, the scattered one varied from less than 6% (position 6) to 7.5% (position 1). When plotting the un-collided normalised count against the detector position, the profile “Experimental” in Fig. 4 is obtained. Uncertainties on these data (not shown in the figure for a better readability) are of order $\pm 3\%$ and arise from the quadratic combination of the counting statistics ($\pm 1\%$) and the detector-to-detector response variability ($\pm 3\%$). Experimental data were unfolded using the FRUIT code [17]. As in the case of the Bonner spheres, the unfolding process is under-determined, as it pretends to determine a multi-group neutron spectrum starting from usually less than ten measurements (the normalised detector counts). Thus, the number of mathematical functions able at reproducing the experimental data is potentially infinite. A way to orientate the unfolding code towards a physically acceptable solution is to complement the unfolding process with some amount of pre-information, in addition to the response matrix, detector counts and related uncertainties. A “realistic” starting spectrum is the classical way to provide such pre-information. The unfolding code will fold the starting spectrum with the response matrix and

Fig. 5 Starting and unfolded spectra

“move” portions of neutron fluence from energy regions to others, attempting to reproduce the measured data. This iterative process has clearly limited energy resolution, so that fine structures such as narrow peaks will not appear in the resulting spectrum if they have not been introduced in the guess-spectrum. By contrast, the appearance of unexpected structures in the resulting spectrum often indicates that an inadequate starting spectrum was chosen. To unfold the data from the current experiment, a previously determined Bonner spheres spectrum [18] was used as starting spectrum. Figure 5 shows the starting spectrum as well as the unfolded one. Both fluence spectra are normalised to one count in the ^3He monitor and refer to a conventional distance of 100 cm, corresponding to the point where the Bonner spheres were exposed in the experiment of Ref. [18]. The FRUIT code was applied in “Special Gradient Method” [19]. NCT-WES was exposed at a different distance (136 cm), and its spectrum was rescaled using the inverse square law to compare with BSS. It should be noted that whilst the BSS spectrum includes the component scattered by bulky metallic supporting structures, NCT-WES one only includes the un-collided one. So the first spectrum was expected to be larger than the second one, as evidenced by the results in Fig. 5. The reported spectra have uncertainties specified bin by bin. FRUIT derives these uncertainties by propagating uncertainties on the input quantities through the unfolding process [19]. A way to evaluate the unfolded spectrum is to apply it to the response matrix, deriving the so-called folded counts, in turn comparing them to the “experimental counts”. This is done in Fig. 4 showing a satisfactory agreement. Uncertainties of the folded counts of order 5% and arise from the quadratic combination of: (1) NCT-WES Monte Carlo modelling ($\pm 2\%$, based on Ref. [6]); (2) distance and alignment ($\pm 4\%$) and (3) unfolding process ($\pm 2.5\%$).

5 Conclusions

Compact accelerator-driven fusion neutron sources are a practical tool in neutron science for a series of applications, but their emission is anisotropic in terms of intensity and energy distribution. An accurate characterisation of such sources would ideally require a directional neutron spectrometer. The novel single-moderator NCT-WES spectrometer is a good candidate for this application as it combines directional response, simultaneous determination of all energy components, easy operation and high sensitivity. To prove its adequacy for the purpose, NCT-WES was used to measure the near-target 3.1 MeV neutron field produced at 0° from the D–D target of the Frascati neutron generator. To account for the non-uniform irradiation condition experienced in the near-target field, a dedicated response matrix was developed. The angular emission and energy distribution were considered constant over the small angle covered by the collimating entrance of the spectrometer. The resulting neutron spectrum is coherent with that previously derived with Bonner spheres. NCT-WES proved to be a promising device for angular spectrometric characterisation of neutron-emitting targets.

Acknowledgements The authors warmly acknowledge Dr. S. Loreti (ENEA) and Dr. G. Pagano (ENEA) for precious discussions. This work has been supported by project ENTER_BNCT from INFN (Commissione Scientifica Nazionale 5) and by Spanish Project PGC2018-093836-B-C21 (MICINN, Spain, cofounded with FEDER). A. Fontanilla and A. I. Castro-Campoy acknowledge the receipt of a fellowship from the ICTP Programme for Training and Research in Italian Laboratories, Trieste, Italy.

Funding Open access funding provided by Ente per le Nuove Tecnologie, l’Energia e l’Ambiente within the CRUI-CARE Agreement.

Data availability This manuscript has associated data in a data repository. [Authors’ comment: The datasets generated during and/or analysed during the current study are not publicly available due patent but are available from the corresponding author on reasonable request.]

Open Access This article is licensed under a Creative Commons Attribution 4.0 International License, which permits use, sharing, adaptation, distribution and reproduction in any medium or format, as long as you give appropriate credit to the original author(s) and the source, provide a link to the Creative Commons licence, and indicate if changes were made. The images or other third party material in this article are included in the article's Creative Commons licence, unless indicated otherwise in a credit line to the material. If material is not included in the article's Creative Commons licence and your intended use is not permitted by statutory regulation or exceeds the permitted use, you will need to obtain permission directly from the copyright holder. To view a copy of this licence, visit <http://creativecommons.org/licenses/by/4.0/>.

References

1. A. Pietropaolo et al., J. Phys. Conf. Ser. **476**, 0120372 (2016)
2. R. Bedogni et al., Nucl. Instrum. Methods A **782**, 35 (2015)
3. R. Bedogni et al., Nucl. Instrum. Methods A **927**, 151 (2019)
4. R. Bedogni et al., Europhys. Lett. **127**, 12002 (2019)
5. A. Pietropaolo et al., Phys. Rep. **875**, 1 (2020)
6. R. Bedogni et al., Europhys. Lett. **134**, 42001 (2021)
7. J. Gomez-Ros et al., Radiat. Meas. **82**, 47 (2015)
8. R. Bedogni et al., Nucl. Instrum. Methods **983**, 164595 (2020)
9. A. Pietropaolo et al., J. Phys. Conf. Ser. **1021**, 012004 (2018)
10. A.V. Alevra, D. Thomas, Radiat. Prot. Dosim. **107**, 37 (2003)
11. P.R. Goncharov, N.N. Bakharev, Plasma Phys. Control. Fusion **62**, 125016 (2020)
12. International Standard Organization, Reference neutron radiations-part 2: calibration fundamentals of radiation protection devices related to the basic quantities characterizing the radiation field, ISO 8529 (2000)
13. R. Bedogni et al., Nucl. Instrum. Methods A **1018**, 165855 (2021)
14. R. Bedogni et al., Nucl. Instrum. Methods A **780**, 51 (2015)
15. C. Werner, MCNP User manual-code version 6.2, Rep La-UR-17-29981 (2007)
16. D.A. Brown et al., Nucl. Data Sheets **148**, 1 (2018)
17. R. Bedogni et al., Nucl. Instrum. Methods A **580**, 1301 (2007)
18. R. Bedogni et al., Nucl. Instrum. Methods A **940**, 302 (2019)
19. K. Amgarou et al., Nucl. Instrum. Methods A **654**, 399 (2011)